



Published in final edited form as:

*Mol Ther.* 2007 October ; 15(10): 1812–1819. doi:10.1038/sj.mt.6300228.

## Treatment of Inflamed Pancreas with Enkephalin Encoding HSV-1 Recombinant Vector Reduces Inflammatory Damage and Behavioral Sequelae

Ying Lu<sup>1</sup>, Terry A McNearney<sup>1,2,3</sup>, Weidong Lin<sup>1</sup>, Steven P Wilson<sup>4</sup>, David C Yeomans<sup>5</sup>, and Karin N Westlund<sup>1,6</sup>

<sup>1</sup>Department of Neuroscience and Cell Biology, University of Texas Medical Branch, Galveston, Texas, USA

<sup>2</sup>Department of Internal Medicine, University of Texas Medical Branch, Galveston, Texas, USA

<sup>3</sup>Department of Microbiology and Immunology, University of Texas Medical Branch, Galveston, Texas, USA

<sup>4</sup>Department of Pharmacology, Physiology and Neuroscience, School of Medicine, University of South Carolina, Columbia, South Carolina, USA

<sup>5</sup>Department of Anesthesiology, Stanford University, Stanford, California, USA

<sup>6</sup>Department of Physiology, University of Kentucky, Lexington, Kentucky, USA

### Abstract

This study assessed the efficacy of pancreatic surface delivered enkephalin (ENK)-encoding herpes simplex virus type 1 (HSV-1) on spontaneous behaviors and spinal cord and pancreatic enkephalin expression in an experimental pancreatitis model. Replication-defective HSV-1 with proenkephalin complementary DNA (cDNA) (HSV-ENK) or control  $\beta$ -galactosidase cDNA (HSV- $\beta$ -gal), or media vehicle (Veh) was applied to the pancreatic surface of rats with dibutyltin dichloride (DBTC)-induced pancreatitis. Spontaneous exploratory behavioral activity was monitored on days 0 and 6 post DBTC and vector treatments. The pancreas, thoracic dorsal root ganglia (DRG, T9-10), and spinal cord (T9-10) were immunostained for met-enkephalin (met-ENK),  $\beta$ -gal, and HSV-1 proteins. Spinal cord was also immunostained for c-Fos, and pancreas was stained for the inflammatory marker regulated on activation, normal T-cells expressed and secreted (RANTES), mu-opioid receptor, and hematoxylin/eosin. On day 6, compared to pancreatitis and vector controls, the DBTC/HSV-ENK treated rats had significantly improved spontaneous exploratory activities, increased met-ENK staining in the pancreas and spinal cord, and normalized c-Fos staining in the dorsal horn. Histopathology of pancreas in DBTC/HSV-ENK treated rats showed preservation of acinar cells and cytoarchitecture with minimal inflammatory cell infiltrates, compared to severe inflammation and acinar cell loss seen in DBTC/HSV- $\beta$ -gal and DBTC/Veh treated rats. Targeted transgene delivery and met-ENK expression successfully produced decreased inflammation in experimental pancreatitis.

### INTRODUCTION

Visceral pain is of great clinical concern and a major morbidity treated by the medical community. Pancreatic pain, present in most patients with pancreatitis or pancreatic cancer,

Correspondence to: Karin N Westlund.

**Correspondence:** Karin N. Westlund High, Department of Physiology, University of Kentucky, MS-609 Chandler Medical Center, Lexington, Kentucky 40536-0298, USA. E-mail: Karin.High@uky.edu.

can be severe and intractable and often responsive only to strong opioids such as morphine. However, over time, patients may develop tolerance to orally or parenterally administered opioids.

An experimental model for pancreatitis has been developed in which dibutyltin dichloride (DBTC), an industrial chemical, is injected into the tail vein. DBTC induces pancreatic inflammation that is easily visualized and graded histologically, as well as nociceptive behaviors both of which are parallel measures of chronic pancreatitis in humans.<sup>1-3</sup> Gene therapy models that encode transgene products utilizing a herpes simplex virus type 1 (HSV-1)-based vector have demonstrated successful synthesis of transgene products with negligible HSV-1 protein detection in non-dorsal root ganglia (DRG) tissues.<sup>4-6</sup> Replication-deficient HSV-1 vectors encoding human preproenkephalin were efficacious in reducing nociceptive behaviors in other experimental models and this reduction of nociceptive behaviors was abrogated by pretreatment using intrathecal opiate antagonist naloxone.<sup>4,6-9</sup>

In this study, pancreatitis was induced with DBTC and punctuate applications of replication-defective HSV-1-based vectors with proenkephalin complementary DNA (cDNA) (HSV-ENK), control  $\beta$ -galactosidase cDNA (HSV- $\beta$ -gal, DZ), or media vehicle alone (Veh) were given the same day to the pancreatic surface of laparotomized male Lewis inbred rats. This method targeted pancreatic neuronal endings for adsorption of the viral vector and subsequent neuronal delivery of the transgene products. Spontaneous exploratory behavior reflecting ongoing pain was monitored on day 0 (baseline) and day 6. On day 7, immunohistochemical staining for tissue met-ENK,  $\beta$ -gal, HSV-1 protein, c-Fos and regulated on activation, normal T-cells expressed and secreted (RANTES) expression was also assessed.

## RESULTS

### Behavioral studies

Changes in spontaneous exploratory behavior used in experimental pain models are related to level of discomfort and general health/malaise.<sup>10-12</sup> Rats were assessed at day 0 before induction of pancreatitis with DBTC and surface application of vector (Figure 1). Animals were re-tested on day 6 at the peak of hypersensitivity and inflammatory response determined by us for this model previously.<sup>3</sup> Compared to sham surgical animals, animals with pancreatitis receiving either vehicle (DBTC/Veh) or HSV- $\beta$ -gal treatment (DBTC/HSV- $\beta$ -gal) had significantly fewer rearing events and light grid beam breaks; decreased rearing duration, distance traveled, and active time; and significantly increased resting time. We previously reported this complex of behavioral changes in animals with another chemically induced pancreatitis with accompanying histology indicative of pancreatic inflammation.<sup>11</sup> In that study, restoration of exploratory behaviors accompanied treatment with agents known to reverse pain-related behaviors.

Most behavioral measures for animals with DBTC-induced pancreatitis receiving HSV-ENK (DBTC/HSV-ENK) were not significantly different from surgical control animals, including values for rearing events, grid beam breaks, active time, and resting time—only duration and distance of travel were reduced. Thus, despite the pancreatitis in these animals, treatment with HSV-ENK provided significant protection.

In control studies, there were no significant differences from baseline for day 6 spontaneous exploratory behaviors after vehicle only tail vein injections. Likewise, pancreatic applications of HSV-ENK, HSV- $\beta$ -gal, or vehicle alone did not affect behavioral activities ( $P > 0.05$  for all groups, data not shown). Therefore, spontaneous exploratory behaviors were impacted only by the presence of the pancreatitis, which was absent in animals treated with DBTC/HSV-ENK.

## Histopathology study

Morphologic evaluations with blinded histologic grading were performed on the pancreatic tissue from all animals.<sup>13-14</sup> Figure 2 illustrates the pancreas of rats from DBTC/Veh treated (Figure 2b) and DBTC/HSV- $\beta$ -gal treated (Figure 2c) groups revealing extensive pathologic changes, notably tissue edema, exuberant inflammatory cell infiltration, acinar cell atrophy and loss, with corresponding widened inter- and intra-lobular ducts, and extensive periductal fibrosis with disruption of tissue integrity or cytoarchitecture. In striking contrast, pancreas from the DBTC/HSV-ENK treated rats displayed minimal inflammatory cell infiltration, had nearly normal retention of the acinar cells with normal tissue integrity, and negligible fibrosis (Figure 2d). A small amount of tissue edema and widening of the ducts could be appreciated in DBTC/HSV-ENK treated rats when compared to pancreatic tissues derived from naive rats or sham treated control animals (Figure 2a). The histopathology seen with HSV-based treatment alone did not display cytopathic effects that have been reported with one case report of HSV-1 associated pancreatitis,<sup>15</sup> thus the DBTC-induction was required for the inflammatory state (see below).

## Immunohistochemical studies

### HSV-1 expression in the thoracic DRG, but not in the pancreas and spinal cord

—Pancreatic tissues, thoracic and cervical DRG (T9-10, C4-5), and spinal cord (T9-10, C4-5) of rats with different treatments were examined for the presence of HSV-1 proteins using immunocytochemistry (Figure 3). No HSV-1 protein staining was noted in pancreas or liver of the sham control (Figure 3a), DBTC/Veh treated (Figure 3b), DBTC/HSV- $\beta$ -gal treated (Figure 3c), or DBTC/HSV-ENK treated (Figure 3d) animals. Prominent immunoreactivity for HSV-1 proteins was detected in thoracic DRG (T9-10) from DBTC/HSV- $\beta$ -gal (Figure 3g) and DBTC/HSV-ENK (Figure 3h) treated animals but not cervical DRG or spinal cords (Figure 3i and j, respectively). There was no staining in DRG of sham control animals (Figure 3e) or animals with DBTC-induced pancreatitis only (Figure 3f).

### Met-ENK expression in pancreas and spinal cord

**Pancreas:** Met-ENK staining was globally expressed in vesicles of acinar cells in pancreas of DBTC/HSV-ENK treated rats (Figure 4d and e) and was significantly greater than in sham surgery animals (Figure 4a,  $P < 0.05$ ) or DBTC/HSV- $\beta$ -gal (Figure 4c,  $P < 0.01$ ) treated rats. In pancreatic tissue from DBTC/Veh (Figure 4b) and DBTC/HSV- $\beta$ -gal (Figure 4c) treated animals, met-ENK staining was located perivascularly and in the inflammatory cell infiltrates. No staining was evident in liver. Paraffin embedding did not allow significant appreciation of neuronal axons. The fluorescent intensity for the immunocytochemical staining of met-ENK was quantified and compared (Figure 4e).

**DRG:** In all animals, met-ENK staining was negligible in T9-10 DRG sensory neuronal cell bodies. This is related to the rapid export of peptides from the soma to axons and terminal endings.<sup>16</sup> Animals receiving HSV-ENK only had control levels of staining for met-ENK.

**Spinal cord:** Met-ENK staining in laminae I, II of the dorsal horn of the T9-10 spinal cord receiving the densest most dense innervation of pancreatic afferents was significantly increased bilaterally in DBTC/HSV-ENK (Figure 4j and f) and DBTC/HSV- $\beta$ -gal treated animals (Figure 4f and i,  $P < 0.05$ ) compared to sham (Figure 4g and f,  $P < 0.05$ ). Met-ENK staining in the cervical spinal cord of DBTC/HSV-ENK treated rats was at control levels (not shown). No increase in met-ENK staining was noted in sham controls treated with HSV-ENK or HSV- $\beta$ -gal alone.

**Expression of the  $\beta$ -gal control vector**—Immunostaining for  $\beta$ -gal was also performed on these tissues to assess the extent of overexpression in the animals treated with the control virus. Protein expression of  $\beta$ -gal reflected successful infection and control transgene protein synthesis detected as granules in DBTC/HSV- $\beta$ -gal treated animals in T9-10 DRG. This constitutive protein was only rarely seen in the other treatment groups.

**RANTES expression in the pancreas**—The staining for the chemokine RANTES in the pancreas as a marker for inflammatory activity was increased in DBTC/HSV- $\beta$ -gal (Figure 5c) and DBTC/Veh (Figure 5b) treated groups compared to sham treated animals (Figure 5a). RANTES staining was evident in acinar cells and infiltrating inflammatory cells. Much less RANTES staining was detected in pancreas of DBTC/HSV-ENK treated animals (Figure 5d), since there were strikingly fewer infiltrating inflammatory cells.

**c-Fos expression in the spinal cord**—c-Fos is an early intermediate gene product induced by neuronal activity used as a marker of response to noxious stimuli. Figure 6a-d depicts c-Fos staining of the thoracic spinal cord (T9-10). Significantly increased c-Fos expression was observed bilaterally in laminae I-IV of the spinal cord in the DBTC/Veh (Figure 6b, f and i) and DBTC/HSV- $\beta$ -gal treated pancreatic rats (Figure 6c, g and i), compared to those sections derived from sham treated rats (Figure 6a, e and i). In contrast, the c-Fos staining in the spinal cord from DBTC/HSV-ENK treated rats (Figure 6d, h and i) was modest and less intense. Unlike localization of c-Fos in many other previous studies of nociception, c-Fos-labeled cells were predominantly localized in deeper layers of the spinal cord (laminae III-V) and around the central canal in lamina X.

#### **Mu opioid receptor expression in the pancreas**

**Pancreas:** Expression level of mu-opioid receptor was increased in the pancreas for all DBTC treatment groups as has been shown in the complete Freund's adjuvant (CFA) inflammation model.<sup>17,18</sup> Figure 7 depicts mu opioid receptor expression in rat pancreas from sham surgery (Figure 7a), DBTC/Veh (Figure 7b), DBTC/ $\beta$ -gal (Figure 7c), and DBTC/HSV-ENK (Figure 7d) treatment groups. The mu-opioid receptor staining in pancreas of DBTC treated rats was increased in acinar cell regions over that in sham surgical animals. The occasional staining of small cells in the other treatment groups are likely infiltrating cells. The mu opioid receptor staining in the DBTC/HSV-ENK (Figure 7d) treatment group was less dense but more predominantly localized in the nuclei of acinar cells.

## **DISCUSSION**

Previous studies have clearly demonstrated that HSV-based vectors can effectively transfer transgene products and have therapeutic potential.<sup>19-21</sup> Our studies illustrate five important properties of HSV-based vector preproenkephalin transgene product delivery: (i) HSV vector application to visceral tissues focuses delivery of transgenes to DRG of sensory afferents innervating this tissue. (ii) Improved spontaneous exploratory behaviors are noted in DBTC/HSV-ENK treated animals. (iii) Tissue inflammation promotes increased vector-associated transgene product generation and delivery to tissue. (iv) In the presence of the transgene product a significant blunting of the DBTC-induced pancreatic inflammatory response is noted with resultant target tissue preservation. (v) Applications of replication-defective HSV-based vector result in a non-productive infection *in vivo*, as previously reported.<sup>5,7,8</sup>

(i) Superficial pancreatic application of replication-defective HSV-1 vectors delivers the human preproenkephalin transgene to thoracic DRG and ultimately targets delivery of met-ENK back to pancreatic tissue. Seven days after HSV-ENK application, significantly increased met-ENK peptide expression was noted in laminae I and II of the dorsal horn of the T9-10

spinal cord and in the pancreas of animals with DBTC-induced pancreatitis. Met-ENK staining was negligible in the cervical spinal cord and liver, suggesting selectivity for the sensory nerves innervating the pancreas that had adsorbed the HSV-1 nucleocapsid. Opiate peptides are synthesized and released endogenously by vascular cells of inflamed peripheral tissue<sup>22,23</sup> to infiltrating inflammatory cells to inhibit inflammation.<sup>24,25</sup> Our studies concur and provide evidence that local supply of met-ENK can also significantly impact inflammation, histological integrity, and nociceptive behaviors. It is unclear, however, why the DBTC/HSV- $\beta$ -gal group had somewhat more met-ENK expression in spinal cord or why there was more apparent histological disruption in the pancreas than in the vehicle control with pancreatitis.

(ii) Studies have shown that endogenous opiates or other manipulated gene products can affect nociceptive responsivity.<sup>26-30</sup> In some models, the effectiveness of overexpressed met-ENK has been shown to persist despite the known gradual decrease in effectiveness for diminishing neuropathic pain in rats after chronic administration with opiates such as morphine after 7 days.<sup>29</sup> Our data indicate that overexpressed opiate neuropeptide prominently influences nociceptive signaling when delivered directly to the target organ, improving spontaneous exploratory behaviors in rats given DBTC/HSV-ENK for at least 7 days.

Nociceptive behavior was assessed with an automated, computer-based behavior box, free from experimenter bias as in a previous pancreatitis pain study.<sup>11</sup> Improved spontaneous exploratory activity among the DBTC/HSV-ENK treated animals was coincident with less c-Fos expression in the T9-10 spinal cord in laminae III-V and X, compared to the inverse for the DBTC/Veh and DBTC/HSV- $\beta$ -gal control groups. This further supports our hypothesis that the observed antinociceptive effects are due to the release of opiates and mediation through opioid receptors. Interestingly, c-Fos staining in the animals with DBTC-induced pancreatitis was localized in deeper laminae of the spinal cord dorsal horn rather than in superficial laminae as in other pain models, *i.e.*, cutaneous and neuropathic pain. Abbadie and Besson speculated in early CFA studies that a deep laminar distribution for c-Fos may denote chronic versus acute noxious activation.<sup>31</sup> We further speculate that deep tissue (or whole body) insults, such as their CFA injections at the base of the tail and pancreatitis in the current study, activate cells deep in the dorsal horn and around lamina X, as opposed to superficial cutaneous insults which activate cells and c-Fos in the superficial dorsal horn. This finding is consistent with demonstrated involvement of the lateral spinothalamic tract cells in laminae IV-V and the post-synaptic dorsal column system with cells of origin in laminae III-V and X, in the transmission of visceral pain.<sup>32</sup>

Previous studies with HSV-ENK viral vectors have demonstrated reversal of the analgesic effects with the opiate antagonist, naloxone.<sup>8,9</sup> It is known that met-ENK is 100 times more potent than morphine as an opiate receptor-mediated inhibitor of adenylate cyclase, but its rapid degradation renders it totally ineffective with systemic administration.<sup>16</sup> One previous study reports met-ENK's potent analgesic action does not lead to tolerance.<sup>27</sup> The physiologic importance of opioid peptides in nociceptive responses is supported by studies involving preproenkephalin knockout mice,<sup>28,29</sup> HSV proenkephalin overexpression in other experimental pain models,<sup>9,30</sup> and morphine block of hyperalgesic behaviors in this pancreatitis model.<sup>3,33</sup>

(iii) Peripheral inflammation may drive synthesis and subsequent delivery of the transgene product, since animals treated with HSV vector application alone, without DBTC-induced pancreatitis, have spontaneous exploratory activities equivalent to the sham group and normal pancreatic histology. The DBTC/HSV- $\beta$ -gal control group had increased met-ENK, reflecting increased endogenous met-ENK release into the spinal cord and pancreatic tissues in response to the pancreatitis model itself.<sup>28</sup> The DBTC/HSV-ENK treated animals, however, have increased intensity of staining for the transgene product significantly over these levels.

(iv) Met-ENK overexpression results in anti-inflammatory effects and tissue preservation. Perhaps the most intriguing finding is the striking diminution of pancreatic inflammation and lack of histologic deterioration in the DBTC/HSV-ENK treated animals. Opioids are typically delivered to inflamed tissues by inflammatory cells; however, in the absence of inflammation, no opioid-containing leukocytes are detected in peripheral tissue.<sup>34</sup> Increases in opiate receptor are dependent on the degree of inflammation.<sup>35</sup> Regional met-ENK delivery and tissue overexpression in the HSV-ENK treated animals is likely derived from the enhanced endogenous release of opiates from both central and peripheral endings of sensory nerves since no HSV protein was evident in the pancreas. The overexpressed met-ENK appears to have a significantly greater protective effect than infiltrating immune cells in the modulation of pain and inflammatory parameters.<sup>35,36</sup>

In CFA arthritis models, animals receiving the HSV-ENK gene encoding viral vectors also sustain significantly less joint destruction and periarticular osteopenia by radiographs, compared to arthritis control animals.<sup>4,8</sup> Anti-inflammatory effects of met-ENK have been previously reported, and it is believed to be the major anti-inflammatory peptide among the preproenkephalin gene products.<sup>36</sup> HSV-1 preproenkephalin transgene therapy studies have shown a 60% reduction of hyperalgesia in a CFA polyarthritis model.<sup>8</sup> An adenoviral-mediated transfer of the interleukin-4 gene also modifies pancreatic invasion of inflammatory cells in this model, including reduction of CD4<sup>+</sup> helper cells.<sup>37</sup>

Blunting of the inflammatory response is also reflected in the decreased RANTES content of the pancreatic tissue of DBTC/HSV-ENK treated rats. The role for neuronal opiates in reduction of inflammation<sup>36</sup> has noted reduction of RANTES in particular.<sup>38,39</sup> The mechanisms of opioid immunosuppression in peripheral target cells are not fully elucidated and may include opioid receptor dependent and independent mechanisms. Mu (morphine), kappa (U50488H), and delta-2 (deltorphin II), but not delta-1 (DPDPE) opioid agonists, have been shown to produce dose-dependent immunosuppressive effects that are blocked by the same selective opioid antagonists, respectively.<sup>40</sup> Data presented here indicate that mu-opioid receptors are overexpressed in pancreatic tissue in this experimental pancreatitis model, as has been shown for DRG after hindpaw inflammation with CFA.<sup>17</sup> Involvement of these receptors in anti-inflammatory effects is supported by evidence of a 30% reduction of plasma extravasation for mu-opioid agonists in inflammatory models.<sup>41-44</sup>

(v) This model demonstrates a negligible primary infection of the pancreatic tissue or secondary infection of the spinal cord. As expected, HSV-1 proteins were located in DRG. Increased met-ENK staining reflecting transport of met-ENK (endogenous and overexpressed transgene) is noted for both spinal cord and pancreatic tissues. Interestingly, application of HSV-ENK in the absence of pancreatitis produced no met-ENK in the pancreas. Increased ambulatory behaviors in this visceral pain model provide another demonstration of effective HSV-mediated transfer for specific transgene expression after delivery to the DRG. In this example, targeting the pancreas provides site-specific delivery for an amplified therapeutic effect with no spread evident in liver or cervical spinal tissues.

These studies indicate that time is required for incorporation of viral vectors into nerve terminals, for retrograde transport of the viral vector to the DRG, for subsequent peptide production and transport to neuronal endings. Future studies will apply this methodology to chronic pancreatitis models under development to assess efficacy for sustained release of the opiate and potential to evade tolerance.<sup>29</sup> Since large and multiple transgenes can be accommodated by the HSV vector and it can remain dormant for extended periods of time, these properties can be exploited for therapeutic advantage for long-term transgene expression in sensory nerves.<sup>45</sup>

## MATERIALS AND METHODS

### Animals

Experiments were approved by the Institutional Animal Care and Use Committee. Seventy-six male Lewis inbred rats (150-200 g) were used for the study maintained under standard conditions with three rats per cage and given Taklab diet 8626 (Harlan, Indianapolis, ID).

### General procedures

Baseline spontaneous behavioral activity assessments were performed on day 0 in an automated, computer-assisted open-field testing apparatus (San Diego Instruments, San Diego, CA). Afterward, animals anesthetized by isoflurane inhalation received a tail vein injection of vehicle or dibutyltin dichloride (DBTC, Sigma-Aldrich, St. Louis, MO) to induce persistent pancreatitis.<sup>3</sup> The pancreatic surface was then exposed by laparotomy and replication-defective HSV-1 with a human proenkephalin cDNA transgene (HSV-ENK), control  $\beta$ -gal cDNA (DZ, HSV- $\beta$ -gal), or media vehicle,<sup>4</sup> were delivered. The researchers delivering the syringe contents, performing the behavioral experiments and histopathological evaluation were blinded to the specific viral or control contents of the syringes. Spontaneous behavioral activities were measured again on day 6, at the peak of DBTC-induced pancreatitis and hypersensitivity, and tissues were harvested on day 7.

Six experimental groups of rats were compared in these studies: (i) sham surgical controls, with tail vein injection of ethanol/glycerol vehicle and laparotomy only (sham surgery, without application to the pancreatic surface;  $n = 10$ ), (ii) DBTC-induced pancreatitis with punctate application of media vehicle (Veh) to the pancreatic surface (DBTC/Veh,  $n = 9$ ); (iii) DBTC-induced pancreatitis treated with micro-punctate application to the pancreatic surface with HSV- $\beta$ -gal (DBTC/HSV- $\beta$ -gal  $n = 15$ ), and (iv) DBTC-induced pancreatitis treated with punctate application to the pancreatic surface with HSV/ENK (DBTC/HSV-ENK,  $n = 15$ ). Additional controls were examined to assess the safety of the HSV vectors: Tail vein injection with vehicle (95% ethanol, glycerol, 2:3, no DBTC) and punctate application to the pancreatic surface with (v) HSV- $\beta$ -gal (veh/HSV- $\beta$ -gal  $n = 9$ ) or (vi) HSV-ENK (veh/HSV-ENK,  $n = 8$ ).

### Induction of persistent pancreatitis

During isoflurane inhalation anesthesia, pancreatitis was induced by a single tail vein injection of DBTC (8 mg/kg body weight in 250  $\mu$ l).<sup>3</sup> The DBTC was first dissolved in 95% ethanol (2 parts or 100 $\mu$ l), then mixed with glycerol (3 parts or 150 $\mu$ l). Using a multiple syringe pump (Harvard Apparatus 22, Holliston, MA), the DBTC was delivered at a rate of 25 $\mu$ l/min for 10 minutes.

### HSV-1-based vectors

The HSV-1 viral vectors containing a human proenkephalin transgene or  $\beta$ -gal gene (control) have been previously described.<sup>6</sup> The HSV-1 virus vector HSV-ENK was constructed by the insertion of an expression cassette containing the strong constitutive human cytomegalovirus promoter, an SV-40 intron, the human proenkephalin cDNA, and an SV-40 polyadenylation site into a shuttle plasmid containing flanking HSV DNA from the thymidine kinase region (*Sna*BI insertion site). The linearized shuttle plasmid and *Pac*I-digested DNA from virus DPZ was co-transfected into the complementing 7B cell line and recombinants selected by limiting dilution as described.<sup>46</sup> This virus is similar to another proenkephalin-encoding virus reported previously to attenuate formalin-induced nociception and potentiate benzodiazepine anxiolysis when injected into the central nucleus of the amygdala.<sup>47,48</sup> Generation of the control virus encoding  $\beta$ -gal under control of the human cytomegalovirus promoter (named DZ or SHZ.1) has been described.<sup>49</sup> These recombinant viral vectors designed for gene therapy are

replication-defective, created using the KOS strain of HSV with both copies of the ICP4-coding region (*IE3* gene) deleted. The inserted genes are under the control of a strong constitutive human cytomegalovirus promoter, allowing expression of inserted gene product at an intracellular locale, in the absence of productive HSV-1 infection *in vivo* and without integration into the host genome.<sup>4</sup> These recombinant viral vectors designed for gene therapy have been rendered replication defective by deletion of the gene encoding ICP4. These vectors do not produce productive viral infection but can persist for months despite negligible viral protein synthesis.

### **Punctate application of viral vectors to pancreatic surface**

Immediately after DBTC injection, rats underwent midline surgical laparotomy to expose the pancreatic surface. Five microliters of HSV-1 media vehicle suspension containing  $2 \times 10^6$  plaque-forming units of the viral vector was diluted (1:10) and applied onto the surface of the pancreas between the pancreatic tissue and the adhered peritoneum, using 1/2 cc U-100 insulin syringe (28G1/2) in two to three areas void of pancreatic duct and blood vessels. Control rats received only a laparotomy. Rats were allowed to recover overnight with free access to fluids. All animals were given 10% ethanol (EtOH) and 5% apple juice in their water for the subsequent 6 days of the experiment to enhance pancreatic irritation as previously described.<sup>1-3</sup>

### **Spontaneous exploratory behavioral activity**

Spontaneous behavioral (exploratory) activities were monitored using an open-field  $16 \times 16$  photo-beam activity system with FLEXFIELD software (San Diego Instruments, San Diego, CA). The photobeam activity system allowed acquisition of movements in *x*, *y*, and *z* axis-orientations within an activity chamber ( $40 \times 40 \times 40$  cm<sup>3</sup>), recording the number of times the photobeam grid system is obstructed. Data were collected in 5-minute intervals for 30 minutes in a blind manner. The ethanol water source was withdrawn and replaced with regular drinking water 20 hours before the photobeam activity system measurement. Control testing indicates no adverse effect in behavioral tests at this time point after removal of ethanolic water.

Six measures of spontaneous behavioral activity at day 0 (baseline) and day 6, the peak of hypersensitivity and inflammation<sup>3</sup> included the number of rearing events, rearing time (seconds), active time (seconds), rest time (seconds), distance traveled (inch), and total counts (number of photobeams broken). Resting time is defined as a period of time when an animal remains in place for 1 second or longer. Comparisons were made among groups for each separate parameter.

### **Histologic preparation and immunohistochemistry**

Rats were anesthetized, the pancreas removed for fixation by immersion (4% paraformaldehyde for 24 hours followed by immersion in 70% ethanol in distilled water), and paraffin sections (4  $\mu$ m) processed for histopathological study. Anesthetized rats were perfused with 4% buffered paraformaldehyde for collection of the thoracic cord and DRG. The animals were then cardiac perfused with 4% buffered paraformaldehyde, and the thoracic and cervical spinal cord, and DRG from T7-12 containing the major source of sensory nerve fibers in the pancreas<sup>50</sup> were collected for immunohistochemical study. After immersion in 30% sucrose/0.1 mol/l phosphate buffer overnight, tissues were frozen embedded and sectioned (30  $\mu$ m thickness).

Frozen sections of thoracic, cervical cord, and DRG and paraffin sections of pancreas were immunostained using rabbit anti-met-ENK serum (met-ENK; Peninsula Lab, San Carlos, CA), rabbit anti- $\beta$ -gal (Cappel, Aurora, OH), and rabbit anti-HSV-1 (HSV-1; DakoCytomation, Carpinteria, CA). Thoracic spinal cord was also stained using polyclonal rabbit anti-c-Fos



(Calbiochem, San Diego, CA). Monoclonal mouse anti-RANTES/CCL5 antibody (R&D Systems, Minneapolis, MN) and rabbit anti-mu opioid receptor antibody (Chemicon, Temecula, CA) were used for de-paraffinized pancreas.

Standard immunohistochemical procedures were used for staining nervous tissue frozen sections and paraffin sections for pancreas. The tissues were incubated with rabbit anti-met-ENK (1:1,000), rabbit anti- $\beta$ -gal (1:1,000), rabbit anti-HSV-1 proteins (1:500), rabbit anti-c-Fos (1:3,000), mouse anti-RANTES (1:100), or rabbit anti-mu opioid receptor (1:4,000).

Semi-quantitative stain intensity values for met-ENK in cord and pancreatic sections were collected using the MetaMorph offline program (Molecular Imaging Systems, Downingtown, PA). The average intensity ( $\pm$ SEM) of met-ENK in lamina I-II of both dorsal horns for each section was taken as a total value. c-Fos labeled cells in both dorsal horns (lamina I-IV) and lamina X were counted manually. Comparisons were made to sham surgery animals for the average of five sections ( $\pm$ SEM). To quantify the met-ENK intensity in the pancreas, staining intensity in rectangular grid region of five random fields was averaged ( $\pm$ SEM) for each animal.

Blinded histopathological examination of the pancreatic tissues was performed with the assistance of Dr. Judith Aronson (Department of Pathology, University of Texas Medical Branch).

### Statistical analysis

Statistical analysis and graph generation were done using GraphPad Prism 4 software (Prism, Irvine, CA). Normal distributions were not obtained with the data collected; therefore the non-parametric Kruskal-Wallis test was used for overall comparisons. The treatment groups were compared to the surgical sham control group using the posthoc Mann-Whitney *U*-tests for behavioral measures, met-ENK intensity and c-Fos cell counts. Means were expressed as average  $\pm$ SEM. A *P* value of  $<0.05$  was considered significant in most cases. For the multiple behavioral outcome measures, we designated *a priori*, active time and resting time as primary variables, based on the results of our previous study.<sup>11</sup> For these two primary measures, a Bonferroni correction was performed, such that  $P < 0.025$  was considered significant.

## ACKNOWLEDGMENTS

The authors wish to thank Judith Aronson, Department of Pathology, University of Texas Medical Branch, for her assistance in grading the pancreatic pathology and Lynette Durant, Department of Neuroscience and Cell Biology, University of Texas Medical Branch, for her excellent secretarial assistance.

## REFERENCES

1. Merkord J, Hennighausen G. Acute pancreatitis and bile duct lesions in rat induced by dibutyltin dichloride. *Exp Pathol* 1989;36:59–62. [PubMed: 2731591]
2. Merkord J, Weber H, Jonas L, Nizze H, Hennighausen G. The influence of ethanol on long-term effects of dibutyltin dichloride (DBTC) in pancreas and liver of rats. *Hum Exp Toxicol* 1998;17:144–150. [PubMed: 9587782]
3. Vera-Portocarrero LP, Lu Y, Westlund KN. Nociception in persistent pancreatitis in rats: effects of morphine and neuropeptide alterations. *Anesthesiology* 2003;98:474–484. [PubMed: 12552208]
4. Wilson SP, Yeomans DC, Bender MA, Lu Y, Goins WF, Glorioso JC. Antihyperalgesic effects of infection with a preproenkephalin-encoding herpes virus. *Proc Natl Acad Sci USA* 1999;96:3211–3216. [PubMed: 10077663]
5. Glorioso JC, Fink DJ. Herpes vector-mediated gene transfer in treatment of diseases of the nervous system (Review). *Annu Rev Microbiol* 2004;58:253–271. [PubMed: 15487938]
6. Wilson SP, Yeomans DC. Virally mediated delivery of enkephalin and other neuropeptide transgenes in experimental pain models. *Ann NY Acad Sci* 2002;971:515–521. [PubMed: 12438172]

7. Wilson SP, Yeomans DC. Genetic therapy for pain management. *Curr Rev Pain* 2000;4:445–450. [PubMed: 11060590]
8. Braz J, Beaufour C, Coutaux A, Epstein AL, Cesselin F, Hamon M, et al. Therapeutic efficacy in experimental polyarthritis of viral-driven enkephalin overproduction in sensory neurons. *J Neurosci* 2001;21:7881–7888. [PubMed: 11588161]
9. Yeomans DC, Lu Y, Laurito CE, Peters MC, Vota-Vellis G, Wilson SP, et al. Recombinant herpes vector-mediated analgesia in a primate model of hyperalgesia. *Mol Ther* 2006;13:589–597. [PubMed: 16288901]
10. Mills CD, Grady JJ, Hulsebosch CE. Changes in exploratory behavior as a measure of chronic central pain following spinal cord injury. *J Neurotrauma* 2001;18:1091–1105. [PubMed: 11686495]
11. Zhang L, Zhang X, Westlund KN. Restoration of spontaneous exploratory behaviors with an intrathecal NMDA receptor antagonist or a PKC inhibitor in rats with acute pancreatitis. *Pharm Biochem Behav* 2004;77:145–153.
12. Martin TJ, Zhang Y, Buechler N, Conkin DR, Eisenach JC. Intrathecal morphine and ketorolac analgesia after surgery: comparison of spontaneous and elicited responses in rats. *Pain* 2005;113:376–385. [PubMed: 15661447]
13. Nevalainen TJ, Aho HJ. Pancreatic grading standards of morphological evaluation and histological grading in experimental acute pancreatitis. *Eur Surg Res* 1992;24:14–23. [PubMed: 1601020]
14. Spormann H, Sokolowski A, Letko G. Experimental acute pancreatitis—a quantification of dynamics at enzymic and histomorphologic levels. *Pathol Res Pract* 1989;185:358–362. [PubMed: 2813189]
15. Shintaku M, Umehara Y, Iwaisako K, Tahara M, Adachi Y. Herpes simplex pancreatitis. *Arch Pathol Lab Med* 2003;127:231–234. [PubMed: 12562243]
16. Gainer, H.; Loh, YP.; Sarne, Y. Biosynthesis of neuronal peptides. In: Gainer, H.; Barondes, SH.; Bloom, F., editors. *Peptides in Neurobiology*. series eds. Plenum Press; New York: 1977. p. 183-219. Current Topics in Neurobiology series
17. Zöllner C, Shaqura MA, Bopaiah CP, Mousa S, Stein C, Schafer M. Painful inflammation-induced increase in  $\mu$ -opioid receptor binding and G-protein coupling in primary afferent neurons. *Mol Pharmacol* 2003;64:202–210. [PubMed: 12869624]
18. Brack A, Rittner HL, Macheltska H, Shaqura M, Mousa SA, Labuz D, et al. Endogenous peripheral antinociception in early inflammation is not limited by the number of opioid-containing leukocytes but by opioid receptor expression. *Pain* 2004;108:67–75. [PubMed: 15109509]
19. Mata M, Glorioso JC, Fink DJ. Gene transfer to the nervous system: prospects for novel treatments directed at diseases of the aging nervous system. *J Gerontol A Biol Sci Med Sci* 2003;58:M1111–M1118. [PubMed: 14684708]
20. DeLuca NA, McCarthy AM, Schaffer PA. Isolation and characterization of deletion mutants of herpes simplex virus type 1 in the gene encoding immediate-early regulatory protein ICP4. *J Virol* 1985;56:558–570. [PubMed: 2997476]
21. Fink DJ, DeLuca NA, Goins WF, Glorioso JC. Gene transfer to neurons using herpes simplex virus-based vectors. *Annu Rev Neurosci* 1996;19:265–287. [PubMed: 8833444]
22. Cadet P, Bilfinger TV, Fimiani C, Peter D, Stefano GB. Human vascular and cardiac endothelia express mu opiate receptor transcripts. *Endothelium* 2000;7:185–191. [PubMed: 10912912]
23. Saeed RW, Stefano GB, Murga JD, Short TW, Qi F, Bilfinger TV, et al. Expression of functional delta opioid receptors in vascular smooth muscle. *Int J Mol Med* 2000;6:673–677. [PubMed: 11078827]
24. Gaveriaux C, Peluso J, Simonin F, Laforet J, Kieffer B. Identification of kappa- and delta-opioid receptor transcripts in immune cells. *FEBS Letters* 1995;369:272–276. [PubMed: 7649271]
25. Bigliardi PL, Buchner S, Ruffli T, Bigliardi-Qi M. Specific stimulation of migration of human keratinocytes by mu-opiate receptor agonists. *J Recept Signal Transduct Res* 2002;22:191–199. [PubMed: 12503615]
26. Meunier A, Latremoliere A, Mauborgne A, Bourgoin S, Kayser V, Cesselin F, et al. Attenuation of pain-related behavior in a rat model of trigeminal neuropathic pain by viral-driven enkephalin overproduction in trigeminal ganglion neurons. *Mol Ther* 2005;11:608–616. [PubMed: 15771963]
27. Gráf L, Migléc E, Bajusz S, Székely JI. Met-enkephalin attenuates morphine tolerance in rats. *Eur J Pharm* 1979;58:345–346.

28. Konig M, Zimmer AM, Steiner H, Holmes PV, Crawley JN, Brownstein MJ, et al. Pain responses, anxiety and aggression in mice deficient in pre-proenkephalin. *Nature* 1996;383:535–538. [PubMed: 8849726]
29. Hao S, Mata M, Goins W, Glorioso JC, Fink DJ. Transgene-mediated enkephalin release enhances the effect of morphine and evades tolerance to produce a sustained antiallodynic effect. *Pain* 2003;102:135–142. [PubMed: 12620604]
30. Yeomans DC, Jones T, Laurito CE, Lu Y, Wilson SP. Reversal of ongoing thermal hyperalgesia in mice by a recombinant herpesvirus that encodes human preproenkephalin. *Mol Ther* 2004;9:24–29. [PubMed: 14741774]
31. Abbadie C, Besson JM. C-fos expression in rat lumbar spinal cord following peripheral stimulation in adjuvant-induced arthritic and normal rats. *Brain Res* 1993;607:195–204. [PubMed: 8481796]
32. Willis, WD.; Westlund, KN. Pain System. In: Paxinos, G., editor. *The Human Nervous System*. 2nd edn.. Amsterdam; Elsevier: 2004. p. 1125-1170.
33. Smiley MM, Lu Y, Vera-Portocarrero LP, Zidan A, Westlund KN. Intrathecal gabapentin enhances the analgesic effects of subtherapeutic dose morphine in a rat experimental pancreatitis model. *Anesthesiology* 2004;101:759–765. [PubMed: 15329602]
34. Machelska H, Cabot PJ, Mousa SA, Zhang Q, Stein C. Pain control in inflammation governed by selectins. *Nat Med* 1998;4:1425–1428. [PubMed: 9846582]
35. Hassan AH, Ableitner A, Stein C, Herz A. Inflammation of the rat paw enhances axonal transport of opioid receptors in the sciatic nerve and increases their density in the inflamed tissue. *Neuroscience* 1993;55:185–195. [PubMed: 7688879]
36. Stein C. Opioid receptors on peripheral sensory neurons. *Adv Exp Med Biol* 2003;521:69–76. [PubMed: 12617565]
37. Brock P, Sparmann G, Ritter T, Jaster R, Liebe S, Emmrich J. Interleukin-4 gene transfer into rat pancreas by recombinant adenovirus. *Scand J Gastroenterol* 2005;40:1109–1117. [PubMed: 16165721]
38. Grimm MC, Ben-Baruch A, Taub DD, Howard OM, Resau JH, Wang JM, et al. Opiates transdeactivate chemokine receptors: delta and mu opiate receptor-mediated heterologous desensitization. *J Exp Med* 1998;188:317–325. [PubMed: 9670044]
39. Hu S, Chao CC, Hegg CC, Thayer S, Peterson PK. Morphine inhibits human microglial cell production of, and migration towards, RANTES. *J Psychopharmacol* 2000;14:238–243. [PubMed: 11106302]
40. Rahim RT, Meissler JJ Jr, Cowan A, Rogers TJ, Geller EB, Gaughan J, et al. Administration of mu-, kappa- or delta2-receptor agonists via osmotic minipumps suppresses murine splenic antibody responses. *Int Immunopharmacol* 2001;1:2001–2009. [PubMed: 11606031]
41. Joris J, Costello A, Dubner R, Hargreaves KM. Opiates suppress carrageenan-induced edema and hyperthermia at doses that inhibit hyperalgesia. *Pain* 1990;43:95–103. [PubMed: 2277720]
42. Binder W, Machelska H, Mousa S, Schmitt T, Riviere PJ, Junien JL, et al. Analgesic and antiinflammatory effects of two novel kappa-opioid peptides. *Anesthesiology* 2001;94:1034–1044. [PubMed: 11465595]
43. Green PG, Levine JD. Delta- and kappa-opioid agonists inhibit plasma extravasation induced by bradykinin in the knee joint of the rat. *Neuroscience* 1992;49:129–133. [PubMed: 1328929]
44. Barber A. Mu- and kappa-opioid receptor agonists produce peripheral inhibition of neurogenic plasma extravasation in rat skin. *Eur J Pharmacol* 1993;236:113–120. [PubMed: 8391450]
45. Burton EA, Fink DJ, Glorioso JC. Replication-defective genomic HSV gene therapy vectors: design, production and CNS applications. *Curr Opin Mol Ther* 2005;7:326–336. [PubMed: 16121698]
46. Primeaux SD, Wilson SP, Cusick MC, York DA, Wilson MA. Effects of altered amygdalar neuropeptide Y expression on anxiety-related behaviors. *Neuropsychopharmacology* 2005;30:1589–1597. [PubMed: 15770236]
47. Kang W, Wilson MA, Bender MA, Glorioso JC, Wilson SP. Herpes virus-mediated preproenkephalin gene transfer to the amygdala is antinociceptive. *Brain Res* 1998;792:133–135. [PubMed: 9593860]
48. Kang W, Wilson MA, Bender MA, Glorioso JC, Wilson SP. Overexpression of proenkephalin in the amygdala potentiates the anxiolytic effects of benzodiazepines. *Neuropsychopharmacology* 2000;22:77–88. [PubMed: 10633493]

49. Mester JC, Pitha PM, Glorioso JC. Antiviral activity of herpes simplex virus vectors expressing murine alpha 1-interferon. *Gene Ther* 1995;2:187–196. [PubMed: 7614249]
50. Won MH, Park HS, Jeong YG, Park HJ. Afferent innervation of the rat pancreas: retrograde tracing and immunohistochemistry in the dorsal root ganglia. *Pancreas* 1998;16:80–87. [PubMed: 9436867]

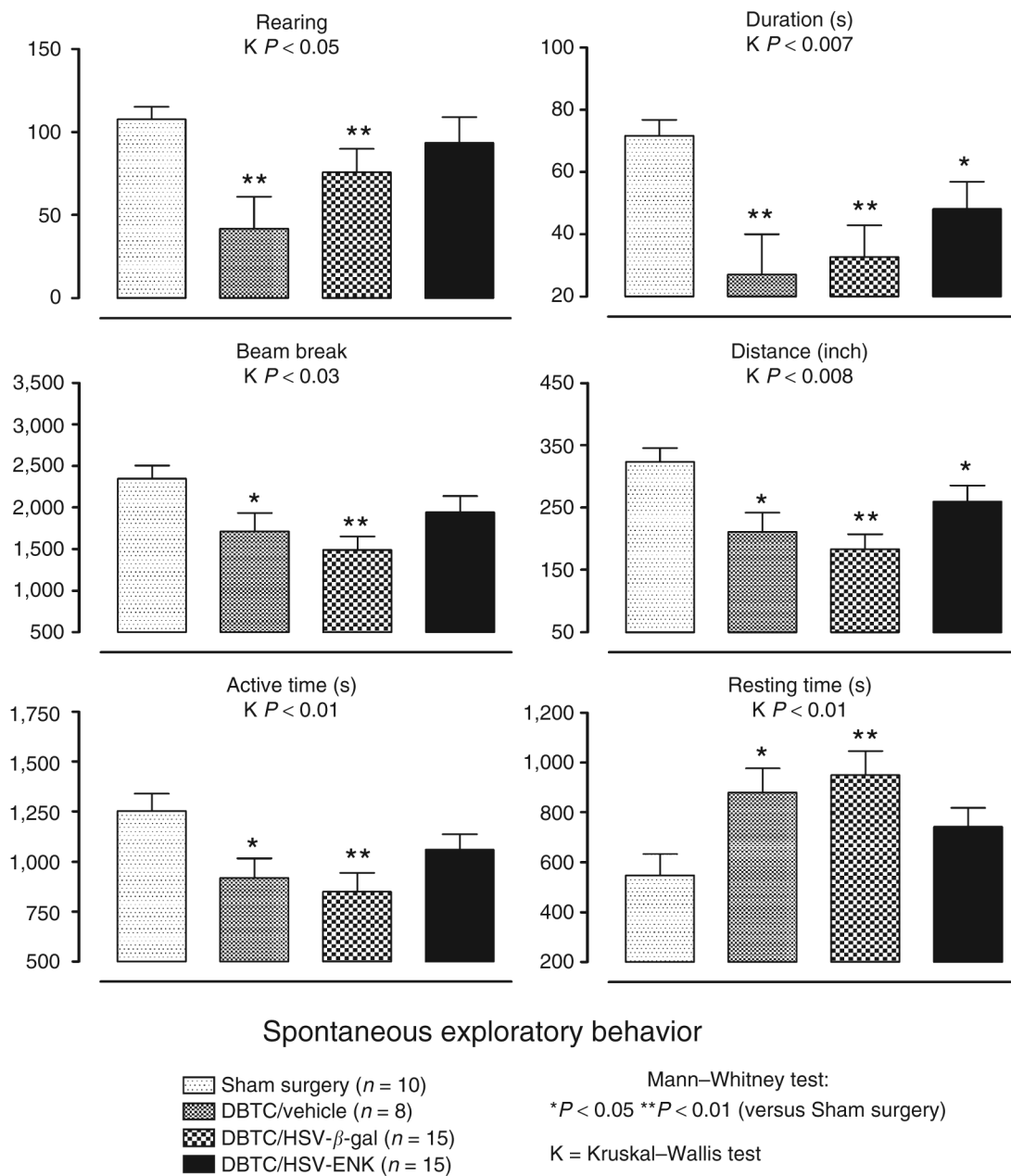


**Figure 1. Spontaneous open-field exploratory behavioral activity measurements in animals with sham surgery or dibutyltin dichloride (DBTC)-induced pancreatitis: rearing events, rearing duration (seconds), total number of light beam brakes, distance traveled (inch), active time (seconds), and rest time (seconds)**

The mean was expressed as average  $\pm$  SEM. The overall comparison using Kruskal-Wallis analysis of variance was significant as indicated (K). \* ( $P < 0.05$ ) and \*\* ( $P < 0.01$ ) indicate significant difference from animals with sham surgery using Mann-Whitney test post hoc comparisons. ENK, enkephalin; HSV, herpes simplex virus.

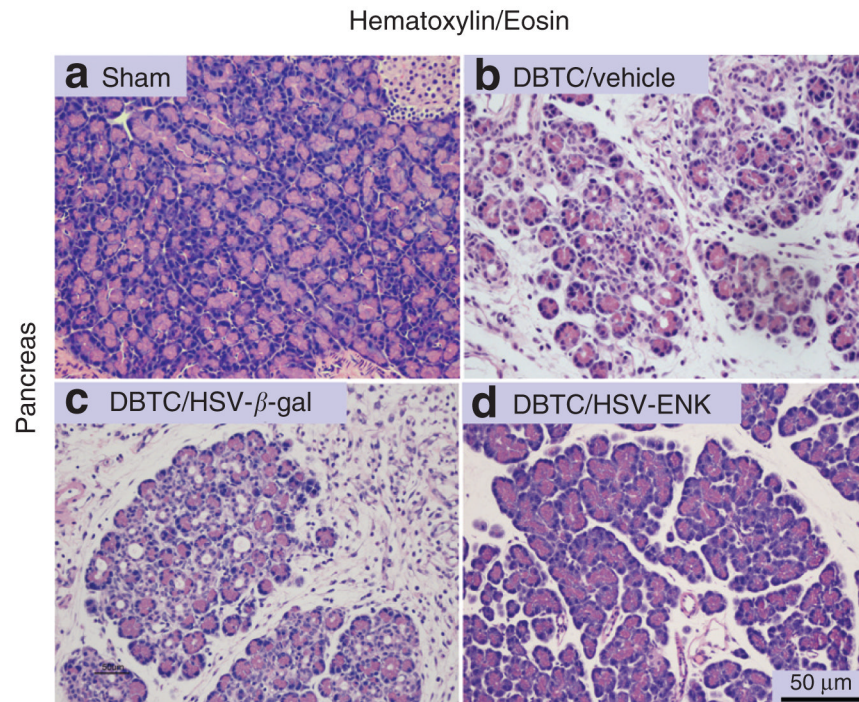


**Figure 2. Photomicrographs depicting the histopathology of rat pancreas**

(a) Pancreas from a rat after sham surgery. (b-d) Pancreas from animals with dibutyltin dichloride (DBTC)-induced pancreatitis treated with the following: (b) vehicle as vector control, (c) HSV- $\beta$ -gal, or (d) HSV-ENK. Note the inflammatory cell infiltration, acinar cell atrophy, widened inter- and intra-lobular ducts, tissue edema and extensive periductal fibrosis seen in DTBC-induced pancreatitis with vehicle or HSV- $\beta$ -gal applications, compared to reduced inflammatory cell infiltration and to preservation of pancreatic tissue architecture in the DTBC and HSV-ENK treated rats. ENK, enkephalin; H&E, hemotoxylin and eosin stain; HSV, herpes simplex virus.

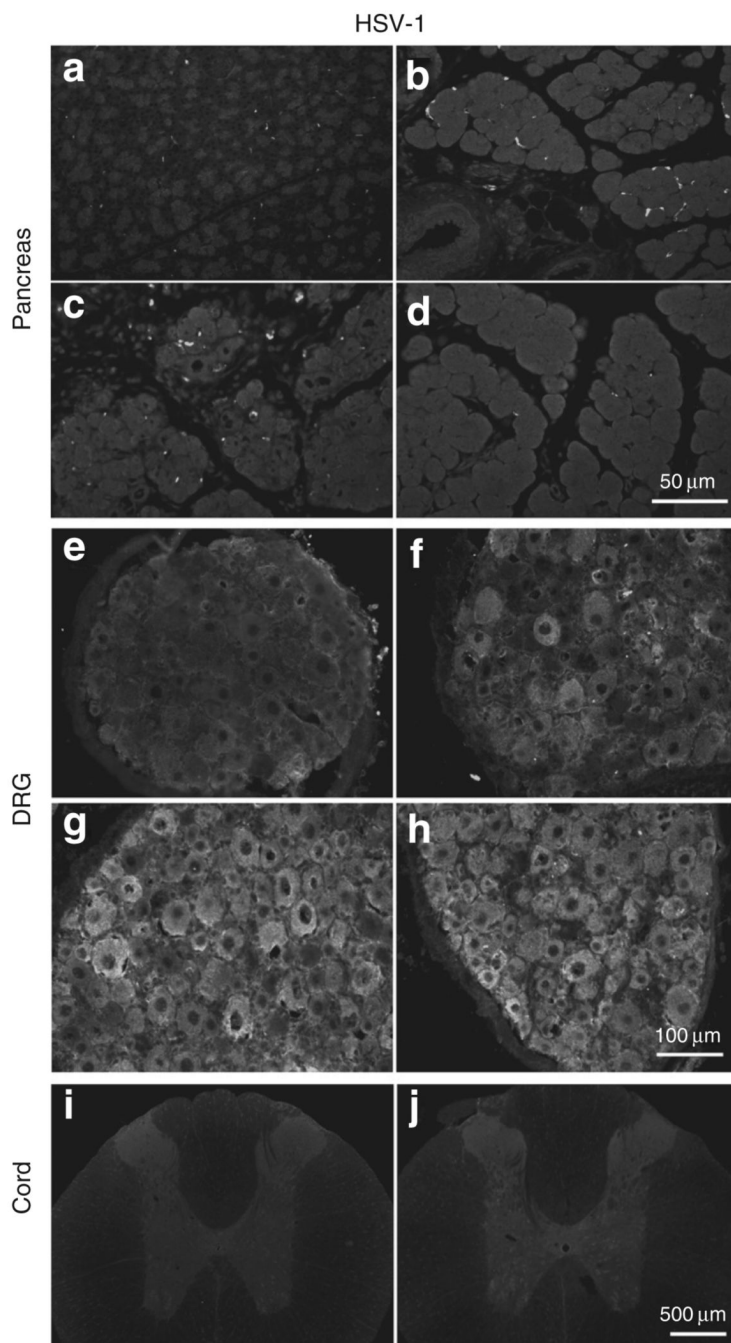


**Figure 3. Photomicrographs of immunohistochemical staining of HSV-1 proteins in pancreas** HSV-1 is shown in (a-d), dorsol root ganglia (DRG, e-h) and spinal cord (i, j) on day 7 of DBTC-induced pancreatitis or in controls. Pancreas after (a) sham surgery and after DBTC-induced pancreatitis with (b) vehicle. (c) HSV- $\beta$ -gal. (d) HSV-ENK. (e) DRG from a rat after sham surgery. DRG from rats with DBTC-induced pancreatitis after application of (f) vehicle. (g) HSV- $\beta$ -gal. (h) HSV-ENK. (i) Spinal cord from a rat after sham surgery. (j) Spinal cord from a rat with DBTC pancreatitis after application of HSV-ENK. ENK, enkephalin.

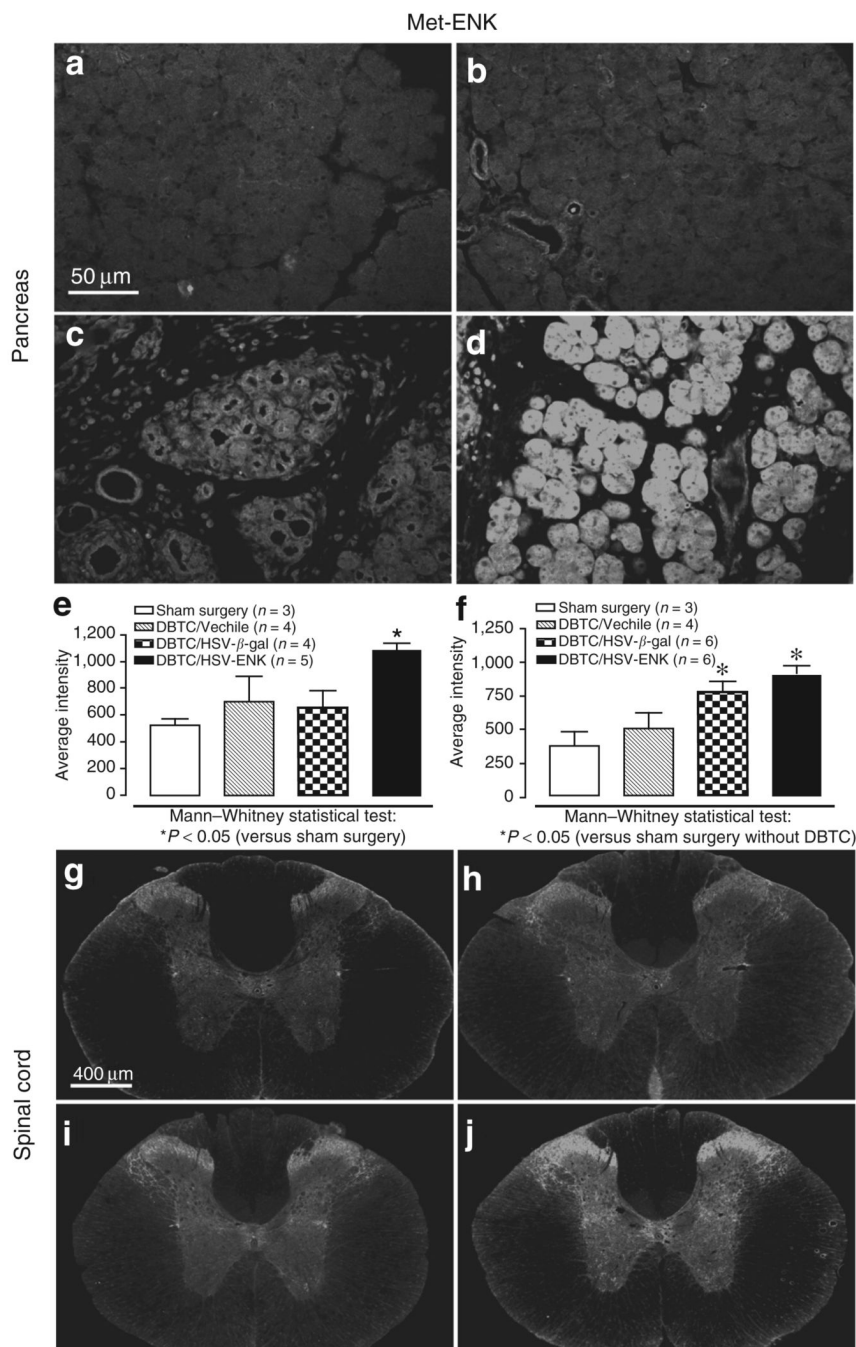


**Figure 4. Photomicrographs of immunohistochemical staining of met-ENK in the pancreas** (a) Pancreas from a rat after sham surgery. (b-e) dibutyltin dichloride (DBTC)-induced pancreatitis and application of (b) vehicle, (c) HSV- $\beta$ -gal as the herpes simplex virus (HSV) vector control, or (d) HSV-ENK. (e) Quantification of fluorescent staining intensity for met-ENK in the pancreas. (f) Quantification of fluorescent staining intensity for met-ENK in the spinal cord. The overall comparisons using Kruskal-Wallis analysis of variance were significant ( $P < 0.05$ ). Significant differences from animals with sham surgery are shown using the Mann-Whitney test for post hoc comparisons. (g-j) Photomicrographs of immunohistochemical staining of spinal cord (T11) met-ENK content. (g) Spinal cord from a rat after sham surgery. (h-j) Spinal cord from animals with DBTC-induced pancreatitis and



application of **(h)** vehicle control, **(i)** HSV- $\beta$ -gal control vector, or **(j)** HSV-ENK. ENK, enkephalin.

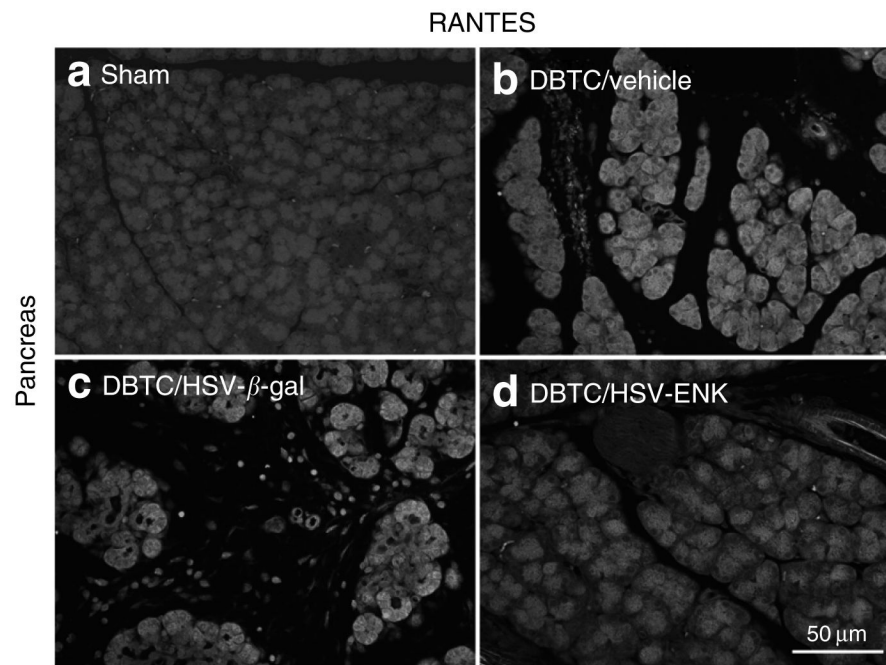


**Figure 5. Photomicrographs of immunohistochemical staining of regulated on activation, normal T cells expressed and secreted (RANTES) in pancreas**  
RANTES in pancreas from animals with (a) sham surgery, and (b-d) dibutyltin dichloride (DBTC)-induced pancreatitis with pancreatic application of (b) vehicle, (c) HSV- $\beta$ -gal as the control vector, or (d) HSV-ENK. ENK, enkephalin; HSV, herpes simplex virus.

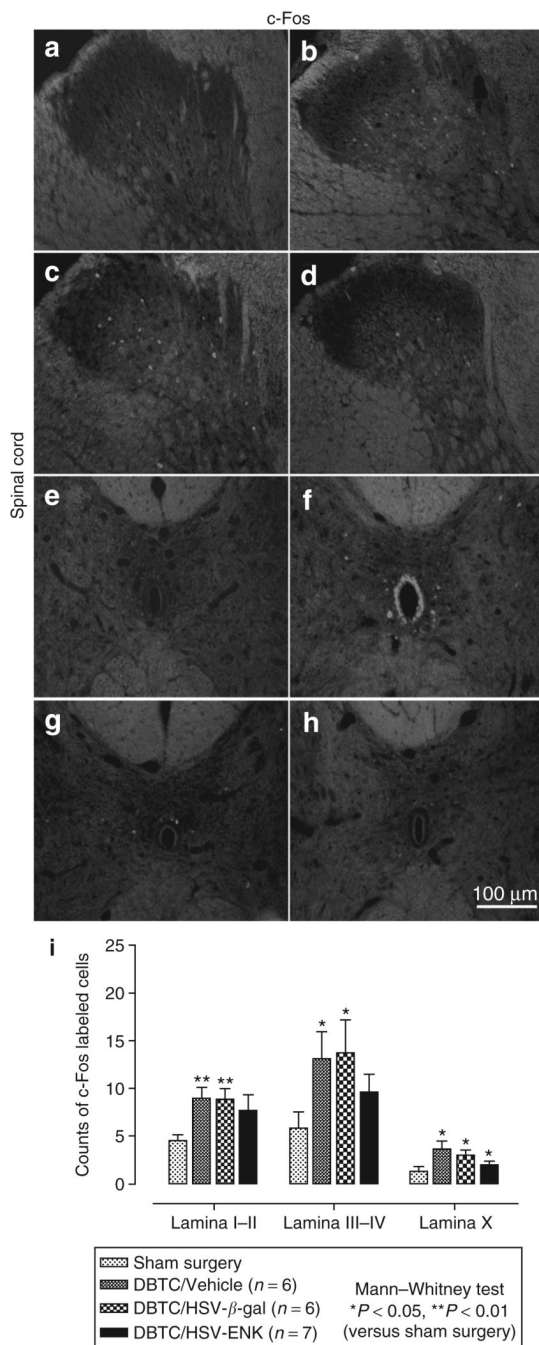


**Figure 6. Photomicrographs of immunohistochemical staining of c-Fos in the dorsal horn of rat thoracic spinal cord (T10)**

The areas corresponding to laminae I-V are shown. (a) Spinal cord from a rat after sham surgery. (b-d) Spinal cord from a rat with dibutyltin dichloride (DBTC)-induced pancreatitis and the following treatments: (b) vehicle, (c) HSV-β-gal as the vector control, and (d) HSV-ENK. Photomicrographs of immunohistochemical staining of c-Fos in lamina X of rat thoracic spinal cord (T10) of a rat after (e) sham surgery, or pancreatic application of (f) vehicle, (g) HSV-β-gal vector control, or (h) HSV-ENK. (i) Quantification of fluorescent c-Fos-labeled cells in spinal cord. The overall comparisons using Kruskal-Wallis analysis of variance were significant ( $P < 0.05$ ). Significant differences in numbers of c-Fos-labeled cells compared to

animals with sham surgery are shown using Mann-Whitney post hoc comparisons. ENK, enkephalin; HSV, herpes simplex virus.

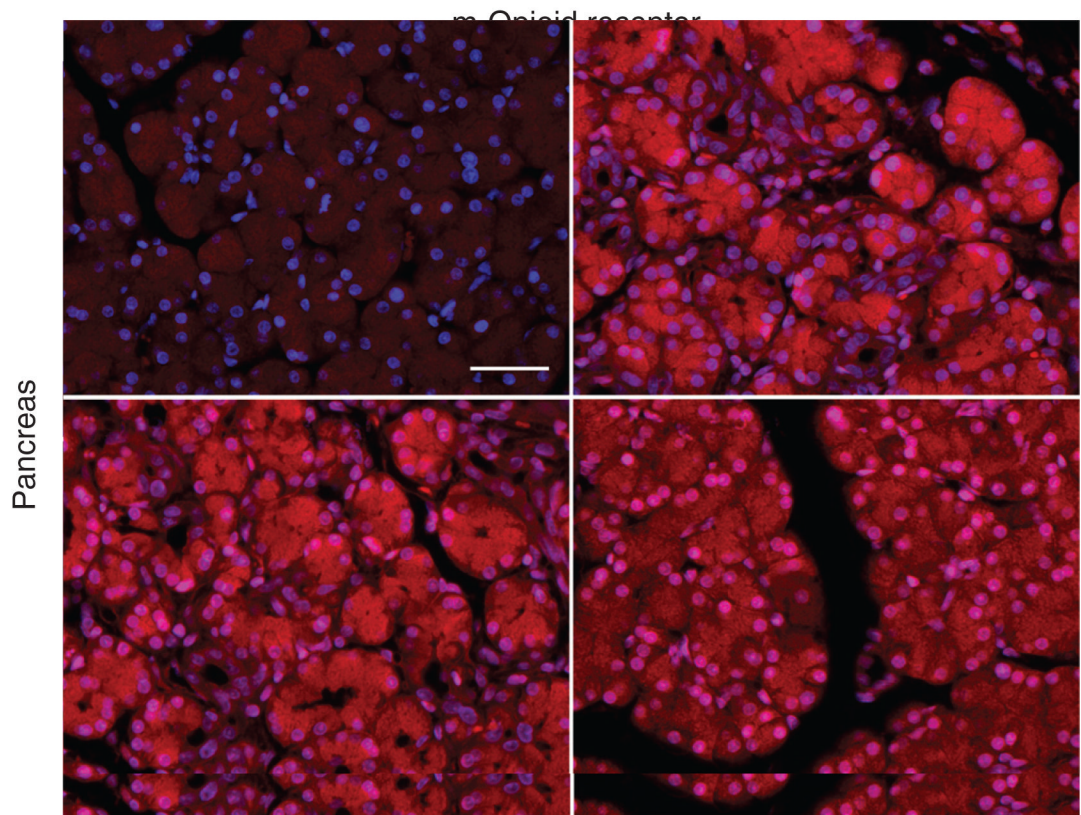


**Figure 7. Immunostaining for  $\alpha$  Mu opioid receptor in rat pancreas**

$\alpha$  Mu opioid receptor is shown after (a) sham surgery or (b-d) dibutyltin dichloride (DBTC)-induced pancreatitis and (b) vehicle, (c) HSV- $\beta$ -gal vector control, or (d) HSV-ENK. The nuclei of cells are counterstained blue by the neutral fluorescent dye 4',6-diamidino-2-phenylindole.